Modeling of Polycyclic Aromatic Hydrocarbon (PAH) Formation during Hydrocarbon Pyrolysis

T. Bensabath[*, 1, 2], H. Monnier[2], C. Champmartin[2], P.-A. Glaude[1]

[1]LRGP, CNRS, Université de Lorraine, Nancy, France
[2]INRS, Vandœuvre-lès-Nancy, France

Abstract
Hydrocarbon pyrolysis in low-pressure gas carburizing conditions drives to gas phase reactions which lead to the production of Polycyclic Aromatic Hydrocarbons (PAHs). These PAHs are afterwards responsible for soot formation. The aim of the study is to predict the formation of mainly sixteen PAHs considered as priority pollutants by the Environmental Protection Agency in the United States (US EPA). Some of them, like benzo(a)pyrene, are carcinogens. A model has been implemented in order to describe the reaction pathways leading to these PAHs. The model was validated using experimental data from the literature, obtained in the case of pyrolysis of different hydrocarbons. Results for ethylene pyrolysis are more specifically presented in this paper. Flux analyses were realized in order to determine the main reaction pathways leading to benzene.

Introduction

Low-pressure gas carburizing is a heat treatment process used to harden surface steel by enriching the metal with carbon atoms coming from the pyrolysis of hydrocarbons. This process is used to avoid wear of pieces subjected to strong constraints [1]. Unfortunately, at the same time, a wide variety of molecules and radicals are also formed in the gas phase. They react between them, leading to the formation of Polycyclic Aromatic Hydrocarbons (PAHs) which are soot precursors [2]. Released into the atmosphere or adsorbed on soot, PAHs are toxic to humans and hazardous to the environment. Sixteen, containing between two and six carbon atom rings, have been classified as priority pollutants by the Environmental Protection Agency in the United States (EPA-PAHs) [3]. Some of them, like benzo(a)pyrene, are known carcinogens [4]. That is why the understanding of PAH formation is important in order to improve the carburizing processes, as other processes which can product PAHs by hydrocarbon pyrolysis or combustion.

There are two main pathways for the formation of the first aromatic rings, benzene and phenyl radical, which are the main actors of PAH growth [5]. The former, the $C_2 - C_4$ way, consists of the addition of an acetylene molecule with a C_4H_5 radical for benzene and with a C_4H_3 radical for phenyl radical [6]. But Miller and Melius estimated that this way cannot be the only one responsible for the first ring formation. Therefore, they proposed another way, the $C_3 - C_3$ way, which consists of the reaction between two propargyl radicals [7]. Cyclopentadienyl radicals also have an important role. Inter alia, they have a part of responsibility in naphthalene formation by addition and recombination of two of them [8].

Although the reactions that lead to the formation of benzene are well known today, the same cannot be said of the reactions that allow the formation of heavier PAHs [5]. PAH growth results from various reaction pathways in competition. The best known is the Hydrogen Abstraction C_2H_2 Addition (HACA) mechanism presented by Frenklach [9]. It consists in the elimination of a hydrogen atom from the initial PAH by a metathesis reaction, followed by the addition of an acetylene molecule on the obtained radical site. This mechanism is an important pathway because of its low energy barrier and its high exothermicity [10]. Other mechanisms were then considered. Among them, there are the combinative growth mechanism which consists in the growth of a PAH by adding aromatic rings, the cyclopentadienyl radical recombination [11] and the Hydrogen Abstraction Vinyl Addition (HAVA) mechanism [12]. Another possible pathway is the Diels-Alder mechanism but it is not competitive with the HACA mechanism [8].

Various models were realized in order to describe reactions which take place during hydrocarbon combustion or pyrolysis until the formation of more or less heavy PAHs. Frenklach et al. developed a model for acetylene and ethylene flames which describes PAH growth to four aromatic rings and soot formation [5, 13]. Slavinskaya et al. worked on a model for methane and ethylene flames and described the PAH growth to five aromatic rings. Their model also allows an estimation of the amount of formed soot [14, 15]. In conditions close to low-pressure gas carburizing, Ziegler realized a model for Chemical Vapor Deposition (CVD) by propane pyrolysis which takes into account the PAH formation to four aromatic rings [16]. The model which considers the heaviest PAHs is the model of Norinaga et al. It details PAH formation up to coronene, that is to say seven aromatic rings. It was validated for ethylene, acetylene and propylene pyrolysis in CVD conditions [17–19], as for propane pyrolysis [20]. Lastly, a model was realized by Matsugi and Miyoshi [21] following studies of pyrolysis of first aromatic rings like toluene [22, 23], allowing to highlight other reaction pathways for PAH formation as

[*] Corresponding author: tsilla.bensabath@univ-lorraine.fr

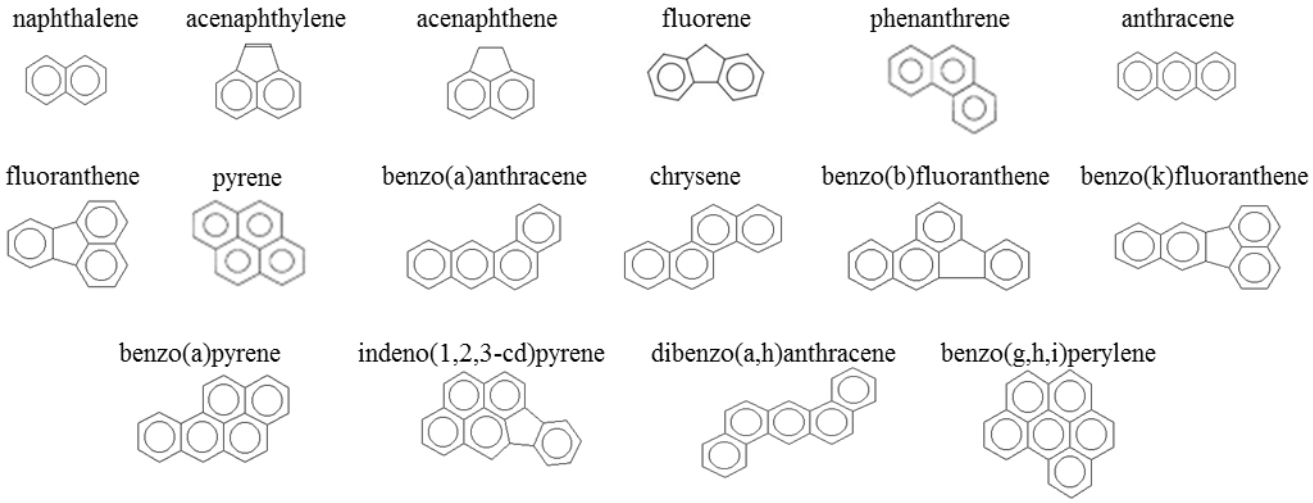

Figure 1: Structures of the 16 EPA-PAHs [3]

the Phenyl Addition and Cyclization (PAC) mechanism.

This study aims to develop a model of hydrocarbon pyrolysis in order to predict the formation of the sixteen EPA-PAHs. These target PAHs are: naphthalene, acenaphthylene, acenaphthene, fluorene, phenanthrene, anthracene, fluoranthene, pyrene, benzo(a)anthracene, chrysene, benzo(b)fluoranthene, benzo(k)fluoranthene, benzo(a)pyrene, indeno(1,2,3-cd)pyrene, dibenzo(a,h)anthracene and benzo(g,h,i)perylene. They are represented in Figure 1.

The establishment of the model is detailed in the next section. Its validation was realized thanks to experimental data from the literature. Data from various sources were used. The first are experimental points coming from propane pyrolysis in a perfectly stirred reactor at 2.6 kPa and for different temperatures between 900 and 1050°C [16]. Next, Sánchez et al. quantified the sixteen EPA-PAHs at the outlet of a plug-flow reactor for acetylene pyrolysis at atmospheric pressure and for different temperatures between 600 and 1050°C [24]. Finally, the latest experimental data come from ethylene, acetylene and propylene pyrolysis in a plug-flow reactor at 8 and 15 kPa and at 900°C [25]. Nevertheless, only the comparison between simulations and these last data for the case of ethylene pyrolysis will be presented in this study. Indeed, differences in reaction pathways are strongly dependent on pyrolysed hydrocarbon for the steps leading to the first aromatic rings, but not for the growth of heavy PAHs [23].

Modeling

A detailed kinetic model for light hydrocarbon pyrolysis and PAH growth has been developed, based on a model of ethylbenzene and anisole combustion [26]. The initial mechanism contained the reactions of pyrolysis and oxidation for hydrocarbons including up to six carbon atoms, the different reaction pathways producing the first aromatic rings from lighter species by $C_2 - C_4$ way, $C_3 - C_3$ way and reactions from cyclopentadienyl radicals, and the reactions of formation of PAHs up to the fourth aromatic ring especially by HACA mechanism. This model has been simplified by removing all oxidation reactions and all species containing oxygen atoms. It has been completed by reactions for the production of heavier PAHs. Other reactions have been added and some kinetic constants have been updated to take into account pathways which could be negligible in the initial oxidation mechanism. The most important changes are detailed in the following. The final model contains 337 species and 1101 reactions.

Among the sixteen EPA-PAHs, six which include two to four rings were already present in the model: naphthalene, acenaphthylene, phenanthrene, anthracene, pyrene and chrysene. Nine have been added with their formation reactions coming from Norinaga et al.'s model [19]: acenaphthene, fluorene, fluoranthene, benzo(a)anthracene, benzo(b)fluoranthene, benzo(k)fluoranthene, benzo(a)pyrene, indeno(1,2,3-cd)pyrene and benzo(g,h,i)perylene. The formation and the consumption of these species involve a significant number of other species which it has been necessary to include in the model. Among them, there are a lot of radical species and other PAHs like acephenanthrylene, benzo(e)pyrene, perylene, anthanthrene or coronene. Lastly, the sixteenth EPA-PAH is dibenzo(a,h)anthracene. To our knowledge, there is no model in the literature which describes pathways leading to it. So, reactions have been written based on these for benzo(a)anthracene, with the same kinetic coefficients. Among them, reactions which directly imply dibenzo(a,h)anthracene or its radicals are reported in Table 1. Figure 2 shows the molecules involved with their corresponding notations. Thermochemical data were evaluated either by analogy with isomers or by the software THERGAS [27].

Using Norinaga et al.'s experimental data for acetylene pyrolysis [25], one notices that the model overpredicted the consumption of acetylene (C_2H_2) as the production of vinylacetylene (C_4H_4), the main primary product of acetylene. The following reaction:

$$C_2H_2 + C_2H_2 \leftrightarrows C_4H_4$$

Table 1: Reactions of formation and consumption of dibenzo(a,h)anthracene (DBAHA3L) and its radicals

phenanthrene + $C_6H_5\#C_2H\bullet$ ⇆ DBAHA3L + H
phenanthrene-2 + $C_6H_5\#C_2H$ ⇆ DBAHA3L + H
BAA3L-9 + C_4H_4 ⇆ DBAHA3L + H
BAA3L-8 + C_4H_4 ⇆ DBAHA3L + H
BEindene• + indenyl → DBAHA3L + H + H
DBAHA3L + H ⇆ DBAHA3L-1 + H_2
DBAHA3L + H ⇆ DBAHA3L-12 + H_2
DBAHA3L + H ⇆ DBAHA3L-4 + H_2
DBAHA3L-1 + H ⇆ DBAHA3L
DBAHA3L-12 + H ⇆ DBAHA3L
DBAHA3L-4 + H ⇆ DBAHA3L
DBAHA3L + CH_3 ⇆ DBAHA3L-1 + CH_4
DBAHA3L + CH_3 ⇆ DBAHA3L-12 + CH_4
DBAHA3L + C_2H_3 ⇆ DBAHA3L-1 + C_2H_4
DBAHA3L + C_2H_3 ⇆ DBAHA3L-12 + C_2H_4
NFindene• + C_5H_5 → DBAHA3L + H + H
BAA3LE-1P + C_2H_2 ⇆ DBAHA3L-1
BAA3LE-2S + C_2H_2 ⇆ DBAHA3L-12

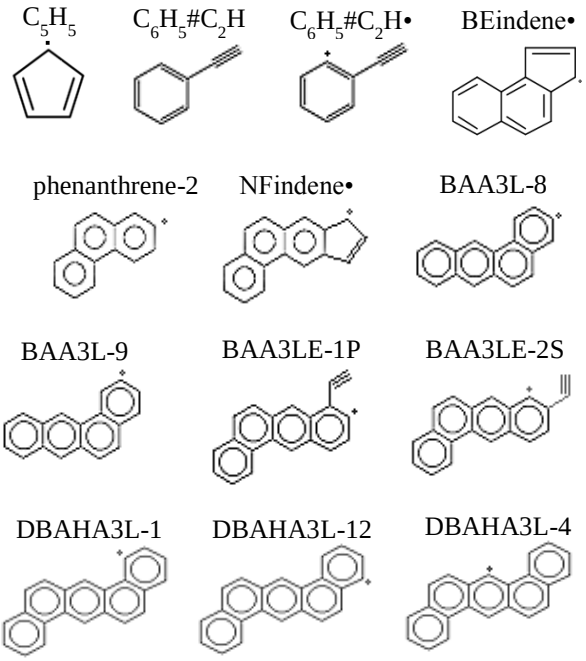

Figure 2: Molecules and radicals involved in Table 1

which was irreversible and thereby too fast, has also been written in reverse direction. Other reactions of vinylacetylene consumption have been added:

$$C_4H_4 + C_2H_2 \leftrightarrows C_6H_6$$
$$C_4H_4 + C_4H_4 \leftrightarrows C_8H_8$$

where C_6H_6 and C_8H_8 represent benzene and 1,3,5,7-cyclooctatetraene respectively. Kinetic coefficients used for these two reactions are Norinaga et al.'s [19]. All these modifications improve prediction of acetylene consumption and of vinylacetylene and benzene production.

Two other reactions written in the direct way only in the initial model have been written reversible:

$$C_7H_7 \leftrightarrows C_5H_5 + C_2H_2$$

$$C_9H_8 + H \leftrightarrows C_7H_7 + C_2H_2$$

This change allows the formation of indene (C_9H_8) from cyclopentadienyl radical (C_5H_5) via benzyl radical (C_7H_7) by successive additions of acetylene molecules. This pathway was not taken into account and improves the prediction by the model of indene production.

Reaction pathways derived from the addition reaction of 1,3-butadiene with vinyl radical were studied by Cavallotti et al. [28]. Two of them have been added in the model with kinetic coefficients proposed by these authors. They are presented in Figure 3. The first one leads to benzene formation and the second one to cyclopentadiene formation. Thermodynamic data of compounds not present in the initial mechanism were evaluated by the software THERGAS [27]. The addition of these reactions especially allows improving prediction of the profiles of 1,3-butadiene and benzene and thereby of most heavier aromatic compounds during ethylene pyrolysis [25].

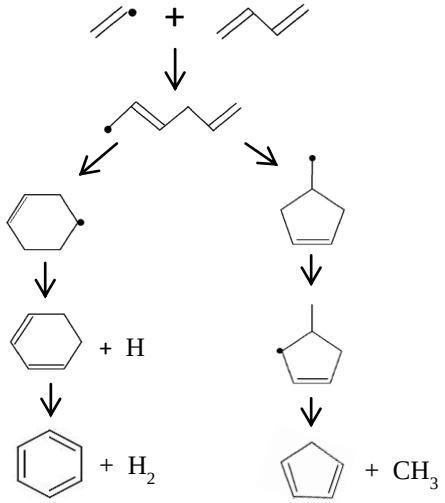

Figure 3: Reaction pathways from addition of 1,3-butadiene and vinyl radical

Because of the presence of acetone in industrial acetylene, five reactions of the decomposition of acetone have been written in the mechanism. They come from Norinaga et al.'s model [19].

Results

The model validation was realized thanks to various experimental data available in the literature. In this section, the concordance of the model with experimental points obtained by Norinaga et al. for ethylene pyrolysis [25] is presented. The inlet stream of the reactor is composed of 99.4% ethylene, 0.4% ethane and 0.2% methane. Measurements were taken at 900°C and at pressures of 8 and 15 kPa, for residence time of 1 s. Simulations were performed using the PSR module in the Chemkin software suite, with the plug-flow reactor represented as a succession of fifteen continuous stirred-tank reactors.

Figure 4 shows results obtained with the model compared with experimental points for ethylene consumption, acetylene, benzene and toluene formation

and lighter EPA-PAH formation at 900°C and 8 kPa. Profiles for heavier EPA-PAHs at 900°C and 15 kPa are presented in Figure 5. Graphs represent the evolution of mole fractions of the different species plotted as a function of the residence time into the reactor. For some PAHs, experimental data are not available. In these cases, the only represented curve is the one obtained by simulation, which allows estimating the order of magnitude for the amount of material of these PAHs.

Curves obtained by simulation agree with experimental points for ethylene, acetylene and benzene. Therefore, the first steps of the pyrolysis are correctly described by the model. In a general way, simulation gives results in correct order of magnitude for PAHs. Some compounds like acenaphthylene, anthracene, benzo(a)anthracene and benzo(a)pyrene are well represented by the model. However, phenanthrene is overestimated and most of other PAHs are underestimated, mainly for significant residence times. This is particularly true for naphthalene, chrysene and benzo(k)fluoranthene.

Otherwise, during experiments of ethylene and acetylene pyrolysis at atmospheric pressure, Sánchez et al. showed that the most formed PAHs are the lightest up to pyrene, except for acenaphthene which is formed in very small quantities [24, 29–31]. These results are generally found here, especially regarding acenaphthene. Nevertheless, there is very little fluorene, suggesting that this compound is underestimated by the model. This conclusion is confirmed by simulating some experiments of Sánchez et al. for acetylene pyrolysis [24] with the model. The results of this simulation are not presented here.

Differences between experimental and modeling results show that some pathways of PAH formation are missing in the model. For example, it is possible that phenanthrene (compound with three aromatic rings) follows reaction pathways which are not taken into account in the model to form pyrene and chrysene (compounds with four aromatic rings). This would explain too high predictions for phenanthrene and too low predictions for pyrene and chrysene. The overestimation of phenanthrene could also be explained by too fast rates of reactions, which allow consuming naphthalene to phenanthrene. This hypothesis is corroborated by the underestimation of naphthalene.

Reaction pathways leading to benzene

It is essential to predict accurately benzene evolution because it is one of the main precursors of heavier PAHs. In the introduction, the main pathways of formation of this aromatic ring described in the literature were recalled. But the model takes into account many other pathways. So, a flux analysis was realized in order to determine the origin of benzene in cases of pyrolysis of different hydrocarbons.

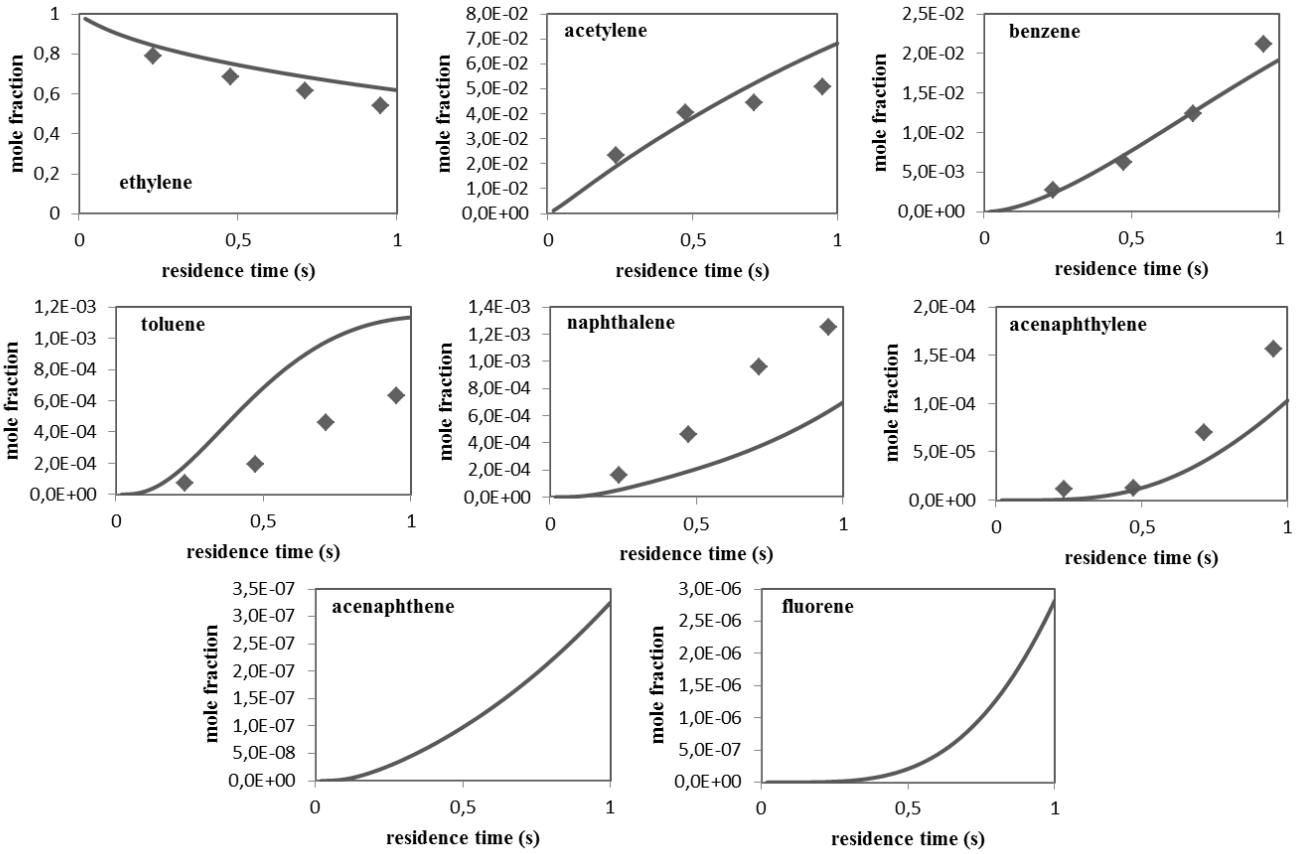

Figure 4: Mole fraction profiles of light species and PAHs during ethylene pyrolysis at T = 900°C and P = 8 kPa [25] Points refer to experiments and lines to the present modeling

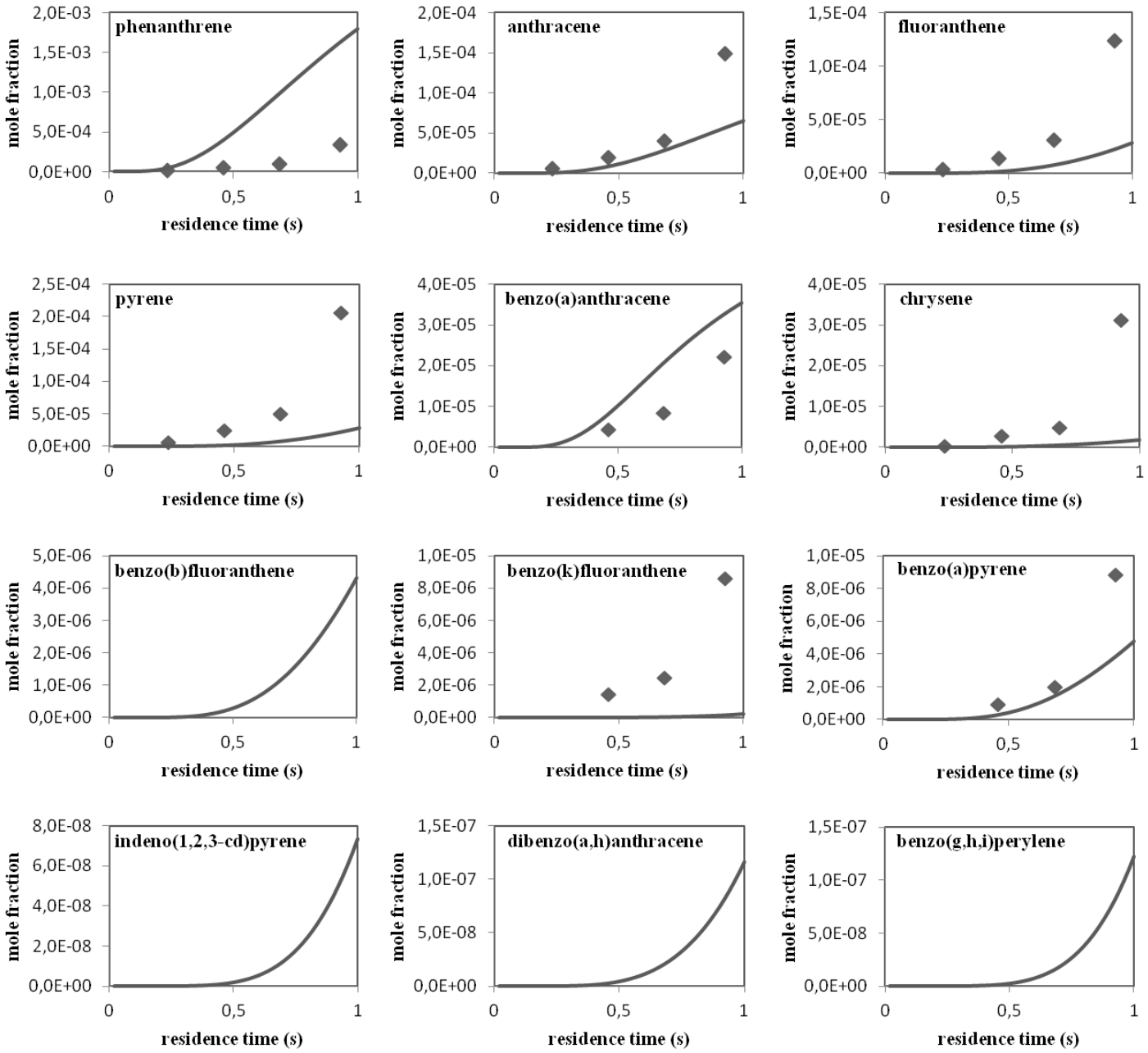

Figure 5: Mole fraction profiles of heavy PAHs during ethylene pyrolysis at T = 900°C and P = 15 kPa [25]
Points refer to experiments and lines to the present modeling

During the simulation of ethylene pyrolysis, two major reaction pathways which are roughly equivalent appear. Both involve 1,3-butadiene. It is one of the major compounds derived from this pyrolysis and it is mainly formed by the addition reaction of vinyl radical on an ethylene molecule:

$$C_2H_4 + C_2H_3 \leftrightarrows 1,3\text{-}C_4H_6 + H$$

The first pathway is the one presented on Figure 3. The second involves fulvene which undergoes an isomerization to turn itself into benzene. Fulvene is mainly formed from iC_4H_5 radical ($H_2C{=}CH{-}C{=}CH_2$) by the following reaction:

$$iC_4H_5 + C_2H_2 \leftrightarrows \text{fulvene} + H$$

iC_4H_5 radical is derived from metathesis reaction of 1,3-butadiene.

As to acetylene pyrolysis, benzene mainly comes from the addition reaction of vinylacetylene with acetylene molecules or vinyl radicals:

$$C_4H_4 + C_2H_2 \leftrightarrows C_6H_6$$
$$C_4H_4 + C_2H_3 \leftrightarrows C_6H_6 + H$$

As to vinylacetylene, it is largely formed by addition of two acetylene molecules, either directly or via diacetylene.

Lastly, the model was used to simulate propylene pyrolysis. In this case, benzene also comes mainly from fulvene isomerization. However, fulvene is formed from propylene thanks to a reaction chain involving different C_3 molecules and radical species. These reactions are the following:

- formation of tC_3H_5 radical ($H_2C=C-CH_3$) from propylene by metathesis
- formation of allene by β-scission of tC_3H_5 radical
- isomerization of allene into propyne
- formation of propargyl radical from propyne by metathesis
- addition of a propargyl radical with an allyl radical to form fulvene.

The different reaction pathways to reach benzene which have been detailed here represent the major pathways for the different pyrolysed hydrocarbons. Nevertheless, other pathways involved to a lesser extent exist. Among them, some involve other cyclic species like methylcyclopentadiene or toluene.

Conclusion

A model to describe the formation of sixteen toxic PAHs during different hydrocarbon pyrolysis has been developed. Depending on the hydrocarbon used, it can more or less describe the evolution of light compounds, although only the ethylene case has been developed here. Regarding the sixteen PAHs, it reproduces reasonably well the orders of magnitude but some compounds are underestimated. This shows that reaction pathways are missing.

Various simulations allowed to highlight the diversity of reaction pathways leading to the first aromatic rings and especially benzene, and to show the strong dependence between pyrolysed hydrocarbon and the predominance of some pathways compared to others. PAH growth is much less dependent on this initial hydrocarbon.

References

[1] K. Yada, O. Watanabe, Comput. Fluids 79 (2013) 65−76.

[2] H. Richter, J.B. Howard, Prog. Energy Combust. Sci. 26 (2000) 565–608.

[3] N.E. Sánchez, A. Callejas, J. Salafranca, Á. Millera, R. Bilbao, M.U. Alzueta, in: F. Battin-Leclerc, J.M. Simmie, E. Blurock (Eds.), Cleaner combustion - Developing detailed chemical kinetic models, Springer, 2013, p. 283−302.

[4] K. Straif, R. Baan, Y. Grosse, B. Secretan, F. El Ghissassi, V. Cogliano, Lancet Oncol. 6 (2005) 931−932.

[5] H. Wang, M. Frenklach, Combust. Flame 110 (1997) 173–221.

[6] P.R. Westmoreland, A.M. Dean, J.B. Howard, J.P. Longwell, J. Phys. Chem. 93 (1989) 8171−8180.

[7] J.A. Miller, C.F. Melius, Combust. Flame 91 (1992) 21−39.

[8] V.V. Kislov, N.I. Islamova, A.M. Kolker, S.H. Lin, A.M. Mebel, J. Chem. Theory Comput. 1 (2005) 908-924.

[9] M. Frenklach, D.W. Clary, W.C. Gardiner Jr., S.E. Stein, Symp. Int. Combust. 20 (1984) 887−901.

[10] V.V. Kislov, A.I. Sadovnikov, A.M. Mebel, J. Phys. Chem. A 117 (2013) 4794−4816.

[11] H. Böhm, H. Jander, Phys. Chem. Chem. Phys. 1 (1999) 3775–3781.

[12] B. Shukla, M. Koshi, Combust. Flame 159 (2012) 3589-3596.

[13] J. Appel, H. Bockhorn, M. Frenklach, Combust. Flame 121 (2000) 122-136.

[14] N.A. Slavinskaya, P. Frank, Combust. Flame 156 (2009) 1705-1722.

[15] V. Chernov, M.J. Thomson, S.B. Dworkin, N.A. Slavinskaya, U. Riedel, Combust. Flame 161 (2014) 592-601.

[16] I. Ziegler, Modélisation cinétique des dépôts de pyrocarbone obtenus par pyrolyse d'hydrocarbures, INPL, Vandœuvre-lès-Nancy, France, 2004.

[17] K. Norinaga, O. Deutschmann, http://www.detchem.com/, 2005

[18] K. Norinaga, O. Deutschmann, Ind. Eng. Chem. Res. 46 (2007) 3547–3557.

[19] K. Norinaga, O. Deutschmann, N. Saegusa, J. Hayashi, J. Anal. Appl. Pyrolysis 86 (2009) 148-160.

[20] R.U. Khan, S. Bajohr, D. Buchholz, R. Reimert, H.D. Minh, K. Norinaga, V.M. Janardhanan, S. Tischer, O. Deutschmann, J. Anal. Appl. Pyrolysis 81 (2008) 148-156.

[21] A. Matsugi, A. Miyoshi, Proc. Combust. Inst. 34 (2013) 269-277.

[22] B. Shukla, A. Susa, A. Miyoshi, M. Koshi, J. Phys. Chem. A 111 (2007) 8308-8324.

[23] B. Shukla, A. Susa, A. Miyoshi, M. Koshi, J. Phys. Chem. A 112 (2008) 2362-2369.

[24] N.E. Sánchez, Á. Millera, R. Bilbao, M.U. Alzueta, J. Anal. Appl. Pyrolysis 103 (2013) 126-133.

[25] K. Norinaga, O. Deutschmann, K.J. Hüttinger, Carbon 44 (2006) 1790-1800.

[26] M. Nowakowska, O. Herbinet, A. Dufour, P.-A. Glaude, Combust. Flame 161 (2014) 1474-1488.

[27] C. Muller, V. Michel, G. Scacchi, G. Côme, J. Chim. Phys. Phys.-Chim. Biol. 92 (1995) 1154-1178.

[28] C. Cavallotti, S. Fascella, R. Rota, S. Carrà, Combust. Sci. Technol. 176 (2004) 705-720.

[29] N.E. Sánchez, A. Callejas, A. Millera, R. Bilbao, M.U. Alzueta, Energy 43 (2012) 30−36.

[30] N.E. Sánchez, A. Callejas, Á. Millera, R. Bilbao, M.U. Alzueta, Energy Fuels 26 (2012) 4823-4829.

[31] N.E. Sánchez, J. Salafranca, A. Callejas, Á. Millera, R. Bilbao, M.U. Alzueta, Fuel 107 (2013) 246-253.